Supporting Information

A Computational Method for Rapid Analysis Polymer Structure and Inverse Design Strategy (RAPSIDY)

Vinson Liao[1], Tristan Myers[1], Arthi Jayaraman[1, 2, *]

1. Department of Chemical and Biomolecular Engineering, University of Delaware, Colburn Lab, 150 Academy Street, Newark, DE 19716
2. Department of Materials Science and Engineering, University of Delaware, 201 DuPont Hall, Newark, Delaware 19716,
3. Data Science Institute, University of Delaware, Ammon Pinizzotto Biopharmaceutical Innovation Center, Suite 147, 590 Avenue 1743, Newark, DE 19713

***Corresponding author:** arthij@udel.edu

1. Definitions of Morphology Densities

In the following section, we define the density fields used to initiate each morphology described in the main text. Each field, φ_A, specifies the number density of type A beads at location (x, y, z) and is fully determined by two parameters: (1) a lattice constant, L_A, which dictates the simulation box size, and (2) the total volume fraction of species A, f_A, for the chosen polymer design. The corresponding density field for bead type B, φ_B, is simply $\varphi_B = 1 - \varphi_A$, by definition. Each field, φ_A, defines a single unit cell of the morphology and can be periodically repeated in the x, y, and z directions. For each morphology, we plot φ_A with a lattice constant L_A=1 and f_A=0.4.

Double Gyroid (DG)[1]

$$\varphi_A(x,y,z,f_A,L_A)=\begin{cases}1, & (x,y,z)\ \in\{\,0<f(x,y,z,L_A)\}\\ 0, & (x,y,z)\ \in\{\,0>f(x,y,z,L_A)\}\end{cases}$$

$$f(x,y,z,f_A,L_A)$$
$$=10\left[cos\left(\frac{2\pi}{L_A}x\right)sin\left(\frac{2\pi}{L_A}y\right)+cos\left(\frac{2\pi}{L_A}y\right)sin\left(\frac{2\pi}{L_A}z\right)+cos\left(\frac{2\pi}{L_A}z\right)sin\left(\frac{2\pi}{L_A}x\right)\right]$$
$$-0.5\left[cos\left(\frac{4\pi}{L_A}x\right)cos\left(\frac{4\pi}{L_A}y\right)+cos\left(\frac{4\pi}{L_A}y\right)cos\left(\frac{4\pi}{L_A}z\right)\right.$$
$$\left.+cos\left(\frac{4\pi}{L_A}z\right)cos\left(\frac{4\pi}{L_A}x\right)\right]-\frac{1-f_A}{0.067}$$

$$x,y,z\ \in\ [0,L_A]$$

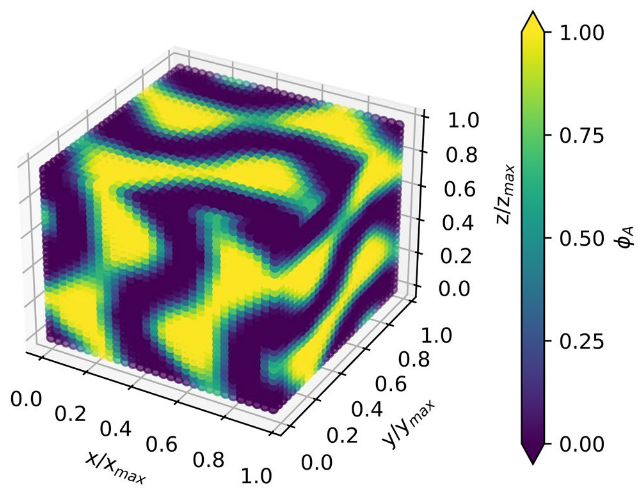

Figure S1. **Density field for double gyroid morphology with a lattice constant, L_A=1, and volume fraction of A, f_A=0.4.**

Lamellar (L)

$$\varphi_A(x,y,z,f_A,L_A) = \begin{cases} 1, & (x,y,z) \in \{\, 0 < f(x,y,z,f_A,L_A)\} \\ 0, & (x,y,z) \in \{\, 0 > f(x,y,z,f_A,L_A)\} \end{cases}$$

$$f(x,y,z,f_A,L_A) = x - f_A * L_A$$

$$x \in [0, L_A]$$

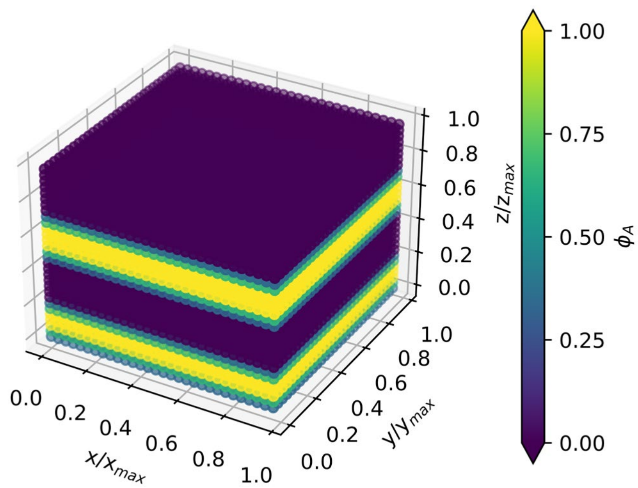

Figure S2. **Density field for lamellar morphology with a lattice constant, L_A=1, and volume fraction of A, f_A=0.4.**

Hexagonally Packed Cylinders (C6)

$$\varphi_A(x,y,z,f_A,L_A) = \begin{cases} 1, & (x,y,z) \in \{ 0 < f(x,y,z,f_A,L_A)\} \\ 0, & (x,y,z) \in \{ 0 > f(x,y,z,f_A,L_A)\} \end{cases}$$

$$f(x,y,z,f_A,L_A) = \min \begin{pmatrix} x^2 + y^2 \\ (x-L_A)^2 + y^2 \\ (x-2L_A)^2 + y^2 \\ (x-\frac{L_A}{2})^2 + (y-\frac{\sqrt{3}}{2}L_A)^2 \\ (x-\frac{3L_A}{2})^2 + (y-\frac{\sqrt{3}}{2}L_A)^2 \\ x^2 + (y-\sqrt{3}L_A)^2 \\ (x-L_A)^2 + (y-\sqrt{3}L_A)^2 \\ (x-2L_A)^2 + (y-\sqrt{3}L_A)^2 \end{pmatrix} - \left(\frac{f_a}{2\pi}\right)^{\frac{2}{3}}$$

$$x, y, \in \ [0, 2L_A], \left[0, \sqrt{3}L_A\right]$$

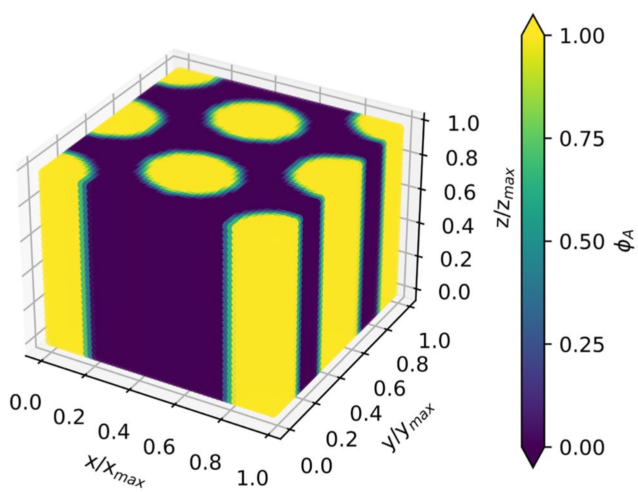

Figure S3. **Density field for hexagonally packed cylinders morphology with a lattice constant, L_A=1, and volume fraction of A, f_A=0.4.**

Body-Centered Cubic (BCC)

$$\varphi_A(x,y,z,f_A,L_A) = \begin{cases} 1, & (x,y,z) \in \{ 0 < f(x,y,z,L_A)\} \\ 0, & (x,y,z) \in \{ 0 > f(x,y,z,L_A)\} \end{cases}$$

$$f(x,y,z,f_A,L_A) = \min \begin{pmatrix} x^2+y^2+z^2 \\ (x-L_A)^2+y^2+z^2 \\ x^2+(y-L_A)^2+z^2 \\ x^2+y^2+(z-L_A)^2 \\ (x-L_A)^2+(y-L_A)^2+z^2 \\ x^2+(y-L_A)^2+(z-L_A)^2 \\ (x-L_A)^2+y^2+(z-L_A)^2 \\ (x-L_A)^2+(y-L_A)^2+(z-L_A)^2 \\ (x-\frac{L_A}{2})^2+(y-\frac{L_A}{2})^2+(z-\frac{L_A}{2})^2 \end{pmatrix} - \left(\frac{f_a}{2\pi}\right)^{\frac{2}{3}}$$

$$x,y,z \in [0,L_A]$$

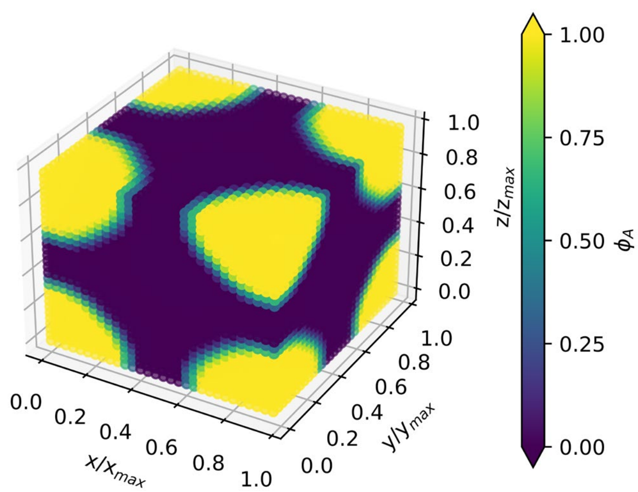

Figure S4. **Density field for body-centered cubic morphology with a lattice constant, L_A=1, and volume fraction of A, f_A=0.4.**

Face-Centered Cubic (FCC)

$$\varphi_A(x,y,z,f_A,L_A)=\begin{cases}1, & (x,y,z)\ \in \{\,0<f(x,y,z,L_A)\}\\ 0, & (x,y,z)\ \in \{\,0>f(x,y,z,L_A)\}\end{cases}$$

$$f(x,y,z,f_A,L_A)=\min\begin{pmatrix} x^2+y^2+z^2\\ (x-L_A)^2+y^2+z^2\\ x^2+(y-L_A)^2+z^2\\ x^2+y^2+(z-L_A)^2\\ (x-L_A)^2+(y-L_A)^2+z^2\\ x^2+(y-L_A)^2+(z-L_A)^2\\ (x-L_A)^2+y^2+(z-L_A)^2\\ (x-L_A)^2+(y-L_A)^2+(z-L_A)^2\\ (x-\frac{L_A}{2})^2+\left(y-\frac{L_A}{2}\right)^2+z^2\\ x^2+\left(y-\frac{L_A}{2}\right)^2+(z-\frac{L_A}{2})^2\\ (x-\frac{L_A}{2})^2+y^2+(z-\frac{L_A}{2})^2\\ (x-\frac{L_A}{2})^2+\left(y-\frac{L_A}{2}\right)^2+(z-L_A)^2\\ (x-L_A)^2+\left(y-\frac{L_A}{2}\right)^2+(z-\frac{L_A}{2})^2\\ (x-\frac{L_A}{2})^2+(y-L_A)^2+(z-\frac{L_A}{2})^2 \end{pmatrix}-\left(\frac{3f_a}{16\pi}\right)^{\frac{2}{3}}$$

$$x,y,z\ \in\ [0,L_A]$$

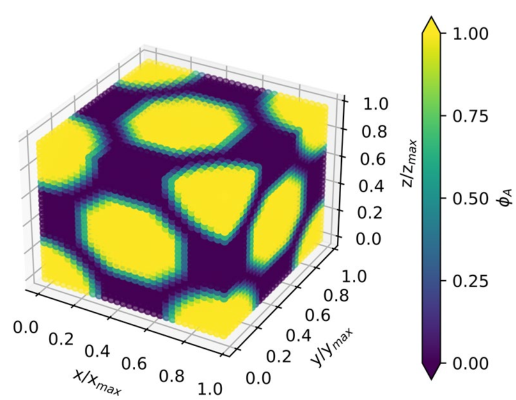

Figure S5. **Density field for face-centered cubic morphology with a lattice constant, L_A=1, and volume fraction of A, f_A=0.4.**

Checkerboard

$$\varphi_A(x, y, z, f_A, L_A)$$
$$= \begin{cases} 1, & if \ \left(0 \le x \le f_A * L_A \ and \ 0 \le y \le \frac{L_A}{2}\right) \ or \ \left((1 - f_A)L_A \ \le x \le L_A \ and \ \frac{L_A}{2} \le y \le L_A\right) \\ 0, & otherwise \end{cases}$$

$$f x, y, z \ \in \ [0, L_A], [0, L_A], [0, L_A]$$

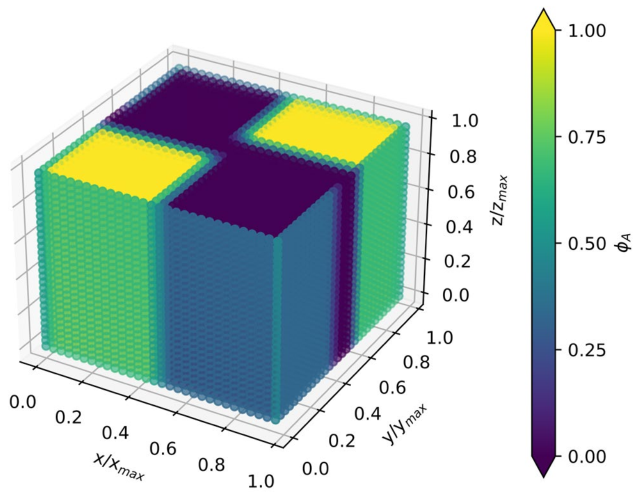

Figure S6. **Density field for checkerboard morphology with a lattice constant, L_A=1, and volume fraction of A, fA=0.4.**

2. Comparison of R_g and R_{ee} distributions from traditional MD versus RAPSIDY

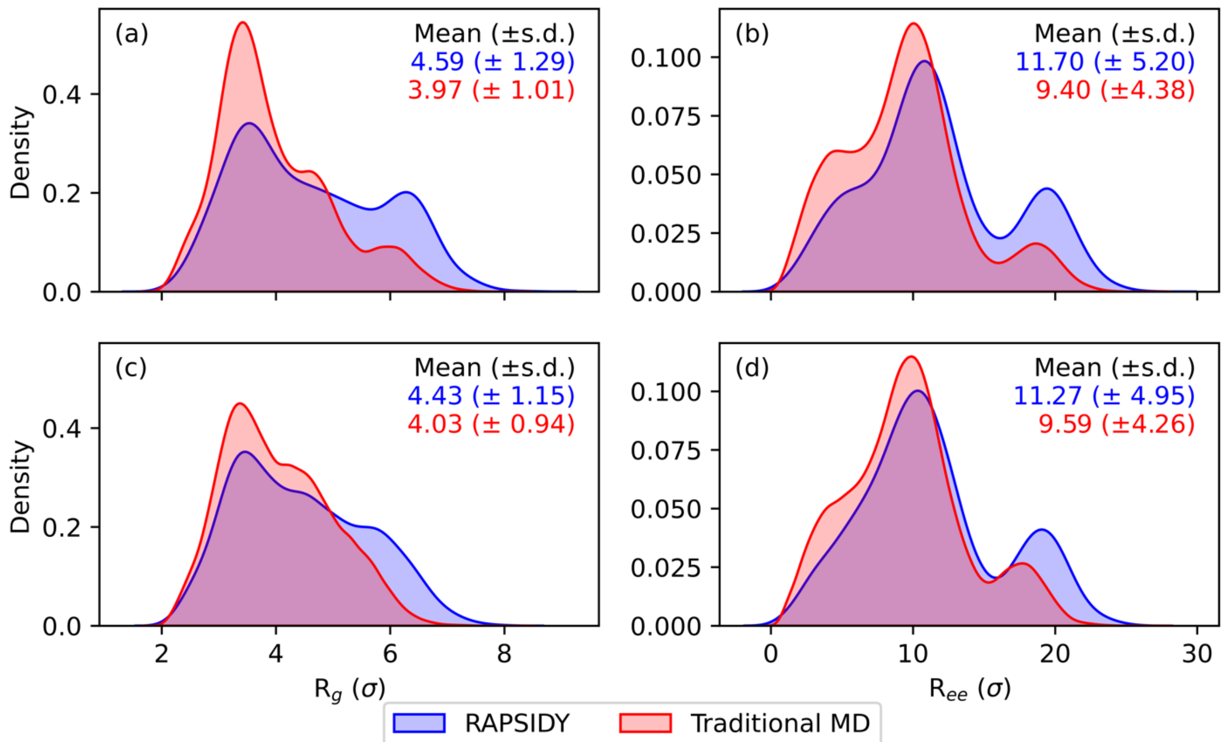

Figure S7. **Comparison of chain level statistics between RAPSIDY and traditional MD for lamellar morphology.** The distributions of the radius-of-gyration and end-to-end distance (in units of σ, in which 1σ is equivalent to the statistical segment length of bead type A and B) are shown in the first and second columns, respectively. The first and second rows correspond go to τ_A=0.4 and τ_A=0.6, respectively, which both form lamellae. Consistency in both the breadth and modality of the distributions suggest that the chain conformations adopted from RAPSIDY and traditional MD are similar.

3. References

1 K.-H. Shen, J. R. Brown and L. M. Hall, *ACS Macro Lett.*, 2018, 7, 1092–1098.